J Mater Sci: Mater Med (2008) 19:2903–2911
DOI 10.1007/s10856-007-3355-4

Synthesis and characterization of nanoporous SiO_2/pHEMA biocomposites

Yen-Yu Liu · Tse-Ying Liu · San-Yuan Chen · Dean-Mo Liu

Received: 2 August 2007 / Accepted: 28 December 2007 / Published online: 18 March 2008

Abstract Porous SiO_2/pHEMA biocomposites were synthesized in situ by incorporating silica nanoparticles with a hydroxyethyl methacrylate (HEMA) monomer, following a UV-induced photopolymerization. The nanostructure of the composites was characterized and the resulting physical properties were examined. The release kinetics of the model molecule—vitamin B12—and the hemocompatibility of the porous SiO_2/pHEMA composites were investigated. Heterogeneous reaction kinetics is proposed to be the formation mechanism of the nanoporosity in the pHEMA matrix as a result of incorporating silica nanoparticles following photopolymerization. Experimental results also demonstrated that the incorporation of the silica nanoparticles into the pHEMA matrix not only enhanced the mechanical property but also maintained a good hemocompatibility of the resulting biocomposites. In addition, it was observed that the drug release profile of the composites (in the form of a membrane) can be precisely regulated from a two-stage pattern to one-stage pattern by varying the concentration of both the SiO_2 nanoparticles and HEMA monomer during synthesis. The permeability of the model drug was enhanced by two orders of magnitude from 4.22×10^{-7} cm^2/h to 3.92×10^{-5} cm^2/h by controlling the micro-to-nanostructure of the composites. The platelet adhesion experiment demonstrated low aggregation of the platelets on the surface of the biocomposite membranes, indicating a promising antithrombotic property.

Y.-Y. Liu · S.-Y. Chen (✉) · D.-M. Liu (✉)
Department of Materials Science and Engineering, National Chiao-Tung University, 1001 Ta-Hsueh Rd, Hsinchu, Taiwan 30010, Republic of China
e-mail: sychen@cc.nctu.edu.tw

D.-M. Liu
e-mail: deanmo_liu@yahoo.ca

T.-Y. Liu
Department of Materials Engineering, MingChi University of Technology, 84 Gungjuan Rd., Taishan, Taipei, Taiwan 243, Republic of China

1 Introduction

Poly(2-hydroxyethyl methacrylate), i.e., pHEMA, has been extensively studied because of its relatively high capability of water uptake, nontoxicity, and favorable compatibility to tissues and blood, which renders itself as an attractive biomaterials for many biomedical applications such as drug delivery vehicles, contact lenses, antithrombotic devices, and implants [1–3]. In order to meet practical requirements, certain properties of pHEMA such as mechanical properties, thermal stability, wettability, diffusion mechanism of solutes (such as biomolecules or drugs), and affinity to specific biomolecules can be tailored and regulated by the incorporation of nanomaterials and manipulated through controlling the composition of inorganic or organic ingredients, nanostructure, nature of inorganic and/or organic components, etc. [4–10].

Silicates are generally considered to be biocompatible and their hybrids or composites have been used in the manufacture of biomedical devices; further, the hemocompatibility of silica hybrids has also been studied [11–13]. Therefore, it is expected that the incorporation of a silica nanophase into the pHEMA matrix can not only enhance the mechanical properties of the resulting composites but also regulate the release kinetics of the drug from within. Until today, the effects of the variation of the structure of the composite on the diffusion characteristics of a molecule, i.e., a drug, have not been systematically

investigated in detail. In addition, the effect of silica nanophase on the hemocompatibility of pHEMA is still unclear.

Many studies have been devoted to the preparation of pHEMA-based composite materials with organic HEMA monomers and inorganic precursors such as tetramethoxysilane (TMOS) or tetraethoxysilane (TEOS) through sol-gel processes [12, 13]. The composite structure of both the inorganic silica and organic pHEMA by either chemical or physical interaction upon in-situ polymerization may offer unique properties that cannot be achieved by individual components. However, upon in-situ sol-gel synthesis of both monomeric inorganic and organic precursors, the presence of organic monomers may retard the hydrolysis and condensation reactions of the inorganic monomers [14]. Moreover, the nonhomogeneous reaction environment caused by processing conditions such as pH value, water concentration, solvent system, and reaction temperature may result in the formation of a nonuniform structure in the resulting composites [15].

In this investigation, SiO_2/pHEMA was synthesized and characterized by directly mixing a well-dispersed silica colloidal suspension with a HEMA monomer following photopolymerization to form a composite structure. This method provides not only a simpler scheme of synthesis to form a SiO_2/pHEMA composite than the aforementioned in-situ synthesis but also avoids the potential drawbacks that originate from the incomplete polymerization of the starting monomeric inorganic components. Further, drug release characteristics can be easily manipulated through the control of nanostructural evolution.

2 Experimental procedures

2.1 Materials

The monomer 2-hydroxyethyl methacrylate (HEMA) (Tokyo Kasei Kogyo Co., Ltd., Japan), the UV photoinitiator benzoin methyl ether (BME) (Tokyo Kasei Kogyo Co., Ltd.), the crosslinking agent ethylene glycol dimethacrylate (EGDMA) (Showa Chemical Co., Ltd., Japan), and nanosilica suspension with particle size ranging from 10 to 12 nm and 20% solid content (ChangChun group, Taiwan) were used for pHEMA and the SiO_2/pHEMA composite synthesis. Vitamin B_{12} (Sigma-Aldrich Co.) was chosen as a model drug to characterize the release profile from the designed composite materials. Phosphate-buffered saline (PBS) (Sigma-Aldrich Co.), glutaraldehyde (Fluka), and alcohol (Aldrich Chemical Co.) were used for the platelet adhesion test. Double-deionized water (by osmosis) was used in the experiments.

2.2 Synthesis of pHEMA and SiO_2/pHEMA composite

The pHEMA and SiO_2/pHEMA composite were prepared by free-radical photopolymerization at room temperature. The content of the HEMA monomer, EGDMA, SiO_2 suspension, and the solvent (H_2O) during the polymerization are summarized in Table 1. The composites of x wt% solvent (H_2O) and y wt% nanosilica particles in the reaction solution are designated as ySixH. The overall nanosilica particles loading was varied in the range of 0–9 wt% for the composites, indicated as "y" in the abbreviations in Table 1. The composition of the composites determines the structure of the resulting composite. The concentrations of the initiator and crosslink agent were 0.1 wt% and 2 wt%, respectively, based on the HEMA weight. The reaction solution was well mixed by an ultrasonic degasser for 5 min. The well-mixed and unseparated reaction solution was injected into a mold and then polymerized to form a composite by UV light exposure at 254 nm for 2 h.

2.3 Characterization

The morphology and structures of the SiO_2/pHEMA composites were examined by field-emission scanning electron microscopy (FE-SEM, JAM-6500F). Microstructure observations were performed using a Philips Tecnai 20 (Holland, The Netherlands) transmission electron microscope operated at 200 keV. The ultrathin sections of the composites were prepared using a Leica EM UC6 Ultramicrotome with EMFCS cryoattachment at room temperature. The cross-sections measuring approximately 100 nm in thickness were obtained by using a diamond knife. The ultrathin films of the composites were directly placed on the copper grids. The tensile mechanical properties of the hybrid composites were measured in wet state by first immersing the composites in water for 2 h and then evaluating through a complete system of MTS Tytron 250 and TestStar IIs systems in a crosshead speed of

Table 1 pHEMA and SiO_2/pHEMA composites

Sample name	HEMA (Wt%)	SiO_2 (Wt%)	H_2O (Wt%)
PHEMA	97.5	0	0
35H	62.5	0	35
50H	47.5	0	50
4Si35H	58.5	4	35
9Si35H	53.47	9	35
2Si50H	45.5	2	50
4Si50H	43.5	4	50
9Si50H	38.5	9	50

10 mm min^{-1} at 25°C. The initial cross section (10 mm^2) was used to calculate the tensile strengths and the tensile modulus. Five parallel measurements were carried out for each sample. The phase transitions of water in the polymer were measured with a differential scanning calorimeter (DSC, Perkin Elmer), equipped with a low-temperature cooling apparatus. The hydrated sample (5–10 mg) was placed in an aluminum pan. The sample was first cooled to −60°C and then heated to 20°C at the rate of 5.0°C/min. The heating process was monitored. The topology of the pHEMA and SiO_2/pHEMA surfaces was studied by atomic force microscopy (AFM) using a NanoScope Multimode atomic force microscope (Digital Instruments, Inc.). The images were recorded with standard tips in contact mode at a scan rate of 1.0 Hz. The root-mean-square (RMS) surface roughness of the membranes was also determined.

2.4 In vitro release kinetics

The procedure for drug release tests has been demonstrated in an earlier study [16]. In brief, the test was performed in a vessel containing two compartment chambers of equal volume; one chamber (considered as the donor side) contained 90 ml of 2,000 ppm vitamin B_{12} in PBS (pH 7.4) and the other chamber was loaded with only drug-free PBS (pH 7.4). Each chamber was mechanically stirred during the test. The concentration of vitamin B_{12} in the medium was measured by a UV-VIS spectrometer (SP-8001; Metertech Inc.) at 361 nm. The permeability was calculated according to Eq. (1) [16]:

$$\ln\left(\frac{C_{10}}{C_1 - C_2}\right) = \frac{2[DH]At}{\delta V} \quad (1)$$

where H is the partition coefficient, D is the effective diffusion coefficient, A is the effective area of the membrane, δ is the thickness of the membrane which was measured by digital thickness gauges (ASTM D926) with five parallel measurements for each sample, V is the solution volume (90 ml), C_{10} is the initial concentration (at $t = 0$) of the drug in the donor solution. C_1 and C_2 are the concentrations in the donor and receptor chambers, respectively, at a given time period ($t = t$) of diffusion. By plotting $\ln[C_{10}/(C_1–C_2)]$ versus time, the permeability $[DH]$ can be obtained from the slope of the line. The apparent partition coefficient (H) of vitamin B_{12} for pHEMA, p(water/pHEMA), and SiO_2/pHEMA composite membranes can be determined as follows [17]. The wet weight (W) of the membranes was recorded after immersing drug-free membranes (1 g) in the release medium (drug-free PBS, pH 7.4) for 2 days. The wet membranes were then immersed in 10 ml of 2,000 ppm vitamin B_{12}−containing medium. The partition coefficient (H) is determined from the initial (C_0) and equilibrium (C_e) concentrations of vitamin B_{12}−containing mediums by Eq. (2):

$$H = 10(C_0 - C_e)/WC_e \quad (2)$$

2.5 Platelet adhesion assessment

The pHEMA and SiO_2/pHEMA composite membranes were equilibrated with PBS for 24 h in a constant-temperature bath. The membranes (1 cm^2) were placed into the 24-well culture plates in contact with 1 ml of human platelet-rich plasma (PRP) and were incubated at 37°C for 1 h. Then, 6 ml of PBS was added to the PRP and retained for 1 min to prevent further platelet adhesion. Adhering platelets were fixed with 2% (w/v) glutaraldehyde solution in PBS at 4°C for 1 h. The platelets fixed on the membrane surfaces were rinsed 3 times with PBS and dehydrated with graded ethanol. They were then characterized by an electron microscope. Five parallel measurements were carried out for each sample.

3 Results and discussion

3.1 Microstructure and physical characterization

Figure 1 shows the cross-sectional microstructure of the SiO_2/pHEMA composites with different amounts of H_2O and SiO_2 concentrations during polymerization. It was observed that, in Fig. 1(a), sample 35H showed a considerably dense and uniform microstructure with no visually observable voids, which is similar to that of pure pHEMA membrane (0H) (not shown in Fig. 1), i.e., without the use of water. However, on increasing the amount of water during the synthesis of pHEMA, i.e., 50H, the resultant samples presented a loose microstructure, as illustrated in Fig. 1(b). This is because although water is a good solvent for the HEMA monomer, it turned to be a poor solvent upon polymerization, i.e., for the HEMA polymer or pHEMA. Phase segregation between water and pHEMA phases may accordingly cause a change in the resultant microstructure. In the presence of water, a transparent, homogeneous pHEMA membrane can be obtained only when the concentration of water is below a certain critical value (between 40% and 60%) [18]. When the water concentration exceeds the critical value, phase separation occurs due to the thermodynamic interaction between water and the polymer network, resulting in an opaque, heterogeneous pHEMA hydrogel.

With the incorporation of the silica nanoparticles together with a sufficient amount of water in the starting solution, the resulting composite membranes of 4Si35H and 4Si50H, shown in Fig. 1(c) and (d), exhibited a wrinkled structure. In contrast to the sample without SiO_2

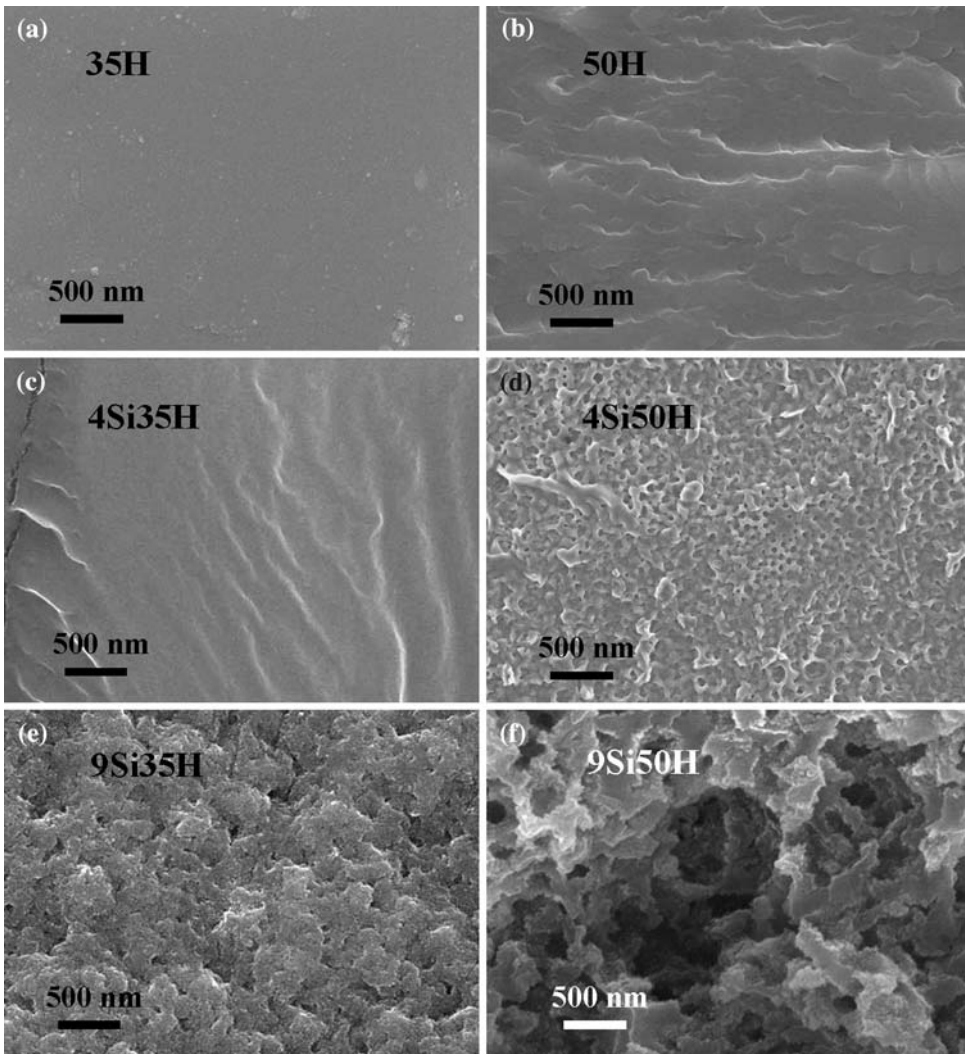

Fig. 1 SEM micrographs of cross-section image of various SiO_2/pHEMA composites

particles, 4Si35H and 4Si50H presented a rougher surface morphology. With a further increase in the content of silica nanoparticles, i.e., sample 9Si35H (Fig. 1(e)) showed a nanoporous structure developed in the composite. Similarly, for sample 9Si50H, with higher water and silica nanoparticles contents, a submicroporous structure was developed, as illustrated in Fig. 1(f), indicating that the addition of SiO_2 nanoparticles induced the formation of nano-to-micro pores. The variation in microstructural evolution of the composites suggests that the presence of the SiO_2 nanoparticles does play an important role in the evolution of nanoporosity during synthesis.

The development of a nanoporous structure in the presence of the nanoparticles suggests that the nanoparticles may act as a heterodomain that induce phase separation, thus forming nanoporosity in the SiO_2/pHEMA composite. As shown in Fig. 1(e), the nanopores developed during UV polymerization were randomly distributed in the composite. These nanopores percolated into a continuous network throughout the composite structure (Fig. 1(f)).

Radical polymerization has been known as the reaction responsible for the synthesis of polymeric HEMA; however, this reaction is expected to take place without interference in the regions at a distance away from the site of the SiO_2 nanoparticles, which is termed as a "bulk region." Nevertheless, in the region (termed "domain region") that is close to the vicinity of the nanoparticles, the polymerization rate of the HEMA monomers is catalytically accelerated over the "bulk region." Thus, the monomers near the silica nanoparticles can be cured at a faster rate under UV irradiation than those of the bulk regions [19–21]. Hence, the difference in the rate of polymerization between the "domain regions" and "bulk regions" induced the formation of heterodomains. It is believed that a phase separation should take place once the heterodomains are fully developed; this would result in a nanoporous structure in the final composite. Furthermore, the diffraction efficiency of the UV light can be enhanced by the presence of nanoparticles [22, 23] so that the presence of SiO_2 nanoparticles is expected to accelerate the

polymerization rate and accordingly, the regions near the nanoparticles polymerize faster than other regions that are far from the nanoparticles is expected. As increasing the content of SiO_2 nanoparticles, it was found that the formation of porous structure of the membranes was enhanced for the samples of 4Si50H and 9Si50H, shown in Fig. 1(d) and (f). In other words, it indicates that the acceleration of polymerization rate could be enhanced by SiO_2 nanoparticles, inducing the phase separation of polymer and the nanoporous structure.

Figure 2 shows that the tensile strength is decreased with increasing water concentration for the samples without silica nanoparticles. This has been explained to be a result of a lower degree of crosslinking during polymerization. However, a considerable improvement in the tensile strength can be detected for the SiO_2/pHEMA composites. It was noted that the tensile strength of the 35H samples increases with the addition of silica nanoparticles up to 4 wt%. This mechanical reinforcement effect of the silica nanoparticles can be referred to an earlier argument where the silica nanoparticles enhanced the degree of polymerization and possibly interacted with the pHEMA matrix although numerous nanopores were formed in the matrix polymer [19]. Those nanopores appear to have little effect on the deterioration of the tensile strength of the 9Si35H composites, and it is believed that the silica nanoparticles do provide an advantage in mechanical reinforcement. The same scenario is prevalent for other compositions except for the sample 9Si50H for which the tensile strength was decreased compared with that of the sample 4Si90H. The explanation for this exception in the sample 9Si50H is due to the water content exceeding a critical value (40%) during the synthesis of SiO_2/pHEMA where a considerable phase separation may have occurred, resulting in a composite with a higher porosity, as evidenced in Fig. 1(f).

A further characterization of the composite materials SiO_2/pHEMA, in comparison to pHEMA, was performed by undertaking swelling experiments. The dried composites and pHEMA were placed in the distilled water and the water uptake was recorded by gravimetric measurement at different time durations. The swelling properties of the composites and pHEMA are shown in Fig. 3, both SiO_2/pHEMA composites of ySi35H and ySi50H series show higher equilibrium swelling than pHEMA. The water absorption of SiO_2/pHEMA composites increases corresponding to the content of silica nanoparticles and the effect is enhanced by increasing the amount of water in the starting reaction solution as illustrated in the ySi50H curves. The swelling ratio of the hydrogel was observed to be dependent on its free volume, the degree of chain flexibility, cross-link density, and hydrophilicity [24]. The change in the swelling ratio might be attributed to the presence of hydrophilic nanosilica in the composite and an enhanced ability of water storage as a result of the nanoporous structure developed in the composites. Thus, an increased swelling ratio can be expected [25].

3.2 Platelet adhesion

Platelet reactivity, measured by the degree of adhesion of platelets to a given surface in vitro, has been proposed as an indication of thrombogenicity for a given material entity. Scanning electron micrographs of the platelet adhesion on pHEMA and SiO_2/pHEMA composite membranes are shown in Fig. 4. Trace amounts of platelets anchored on the surface of the SiO_2/pHEMA composite membrane were detected; these findings closely resembled those observed for the neat pHEMA membrane. A number of surface properties affect platelet adhesion, such as surface roughness, surface charge, and surface energy; the

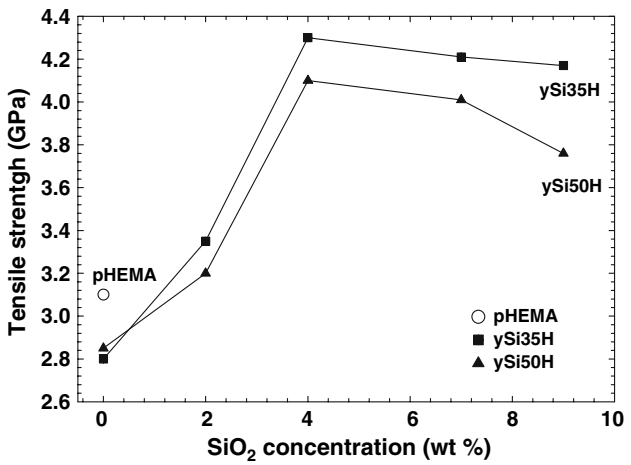

Fig. 2 Mechanical properties of pHEMA and SiO_2/pHEMA composites

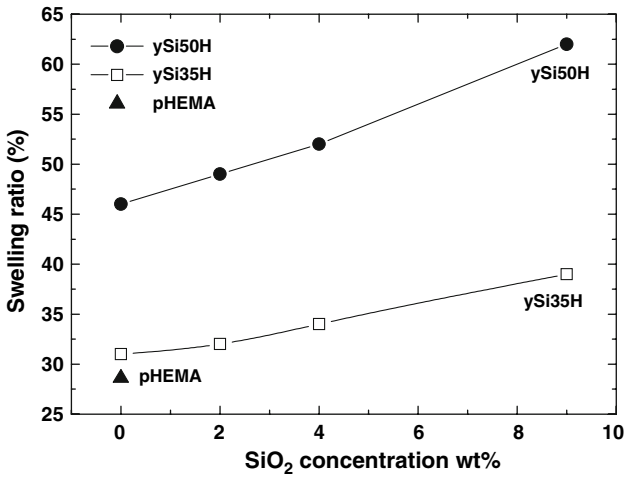

Fig. 3 Amount of water absorption of pHEMA and SiO_2/pHEMA composites

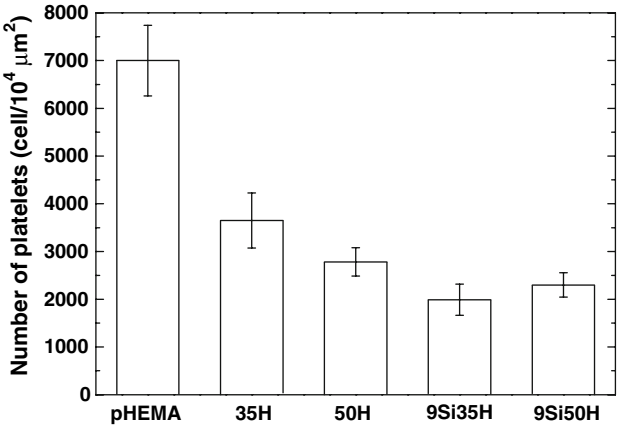

Fig. 4 Number of platelets adhering onto surface of pHEMA and SiO_2/pHEMA membranes

close resemblance between the behavior of platelet adhesion for neat pHEMA and for the composites suggests that these factors may be compromised to some extent with the addition of the SiO_2 nanoparticles and water. From an earlier argument regarding the microstructural evolution following SiO_2 and water incorporation, we examined in particular the surface roughness of the composite surfaces of interest using 3-D AFM, as shown in Fig. 5(a) and (b). The mean square surface roughness (R_a) in a 10 × 10 μm^2 surface region for 35H pHEMA was approximately 56.5 nm; for the 9Si35H composite (i.e., 9 wt% SiO_2 nanoparticles), it increased to 60.8 nm, that is, by a factor of approximately 7.6% compared to that of 35H pHEMA. This finding indicates that the addition of a small amount of SiO_2 nanoparticles into pHEMA had a little or negligible effect on surface roughness. Although no direct evidence can be provided in this investigation for other surface characters, it was believed that the surface properties may remain intact following a small addition of the nanoparticulate phase. This, together with the aforementioned improved properties, encourages the use of such composites for antithrombotic applications.

Furthermore, there has been greater evidence to demonstrate that the water state in polymers exerts a vital role in the biomedical properties of materials [26, 27]. In general, water in a polymer can be classified into three types: nonfreezing water, freezing bound water (cold crystallizable water), and free water [28, 29]. Freezing bound water has been reported to play an important role in hemocompatibility [30]. Therefore, it is important to further confirm whether these SiO_2/pHEMA composites have freezing bound water or not. The water structure in the pHEMA and SiO_2/pHEMA composites as obtained by DSC is disclosed in Fig. 6. In the DSC analysis of pHEMA, the only observed peak is the endothermic one at 2–5°C, assigned to the fusion of ice of free water. In the case of the 9Si35H

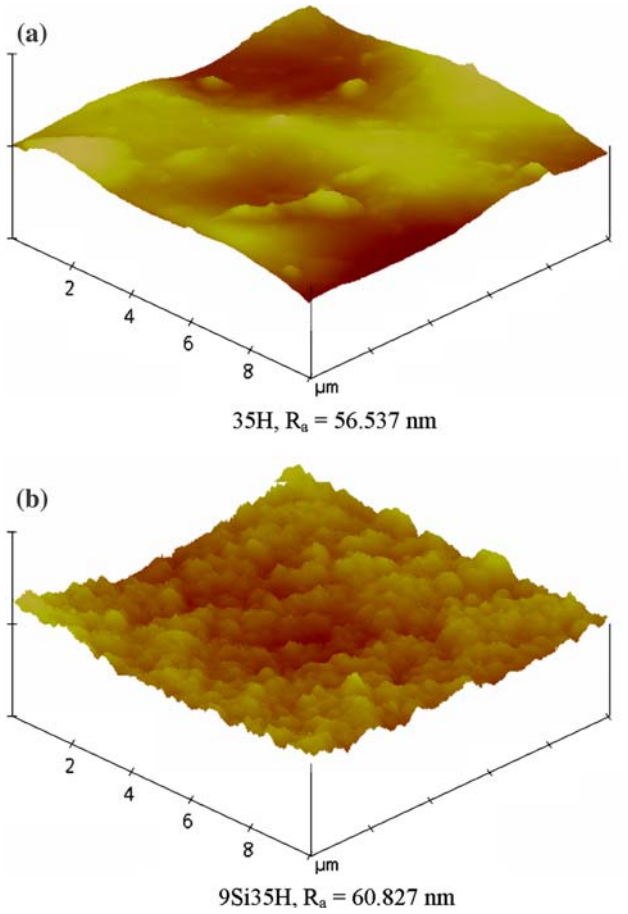

Fig. 5 Tapping-mode AFM images of (**a**) 35H and (**b**) 9Si35H

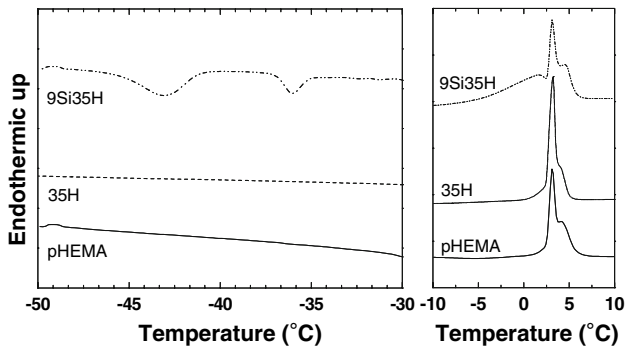

Fig. 6 DSC thermogram of pHEMA and SiO_2/pHEMA composites

composite, two exothermic peaks at −30°C to −50°C and a broad endothermic peak at −5°C to 2.5°C were observed. The typical exothermic peak at −45°C to −35°C (ΔHcc) on heating was assigned to the cold crystallization of water that was defined as freezing bound water [30]. The result of the melting point indicates that the endothermic peak at −5°C to 2.5°C, ΔHm, is assigned to the fusion of ice of cold crystallized water (freezing bound water). Therefore, the water state in the SiO_2/pHEMA composite is composed

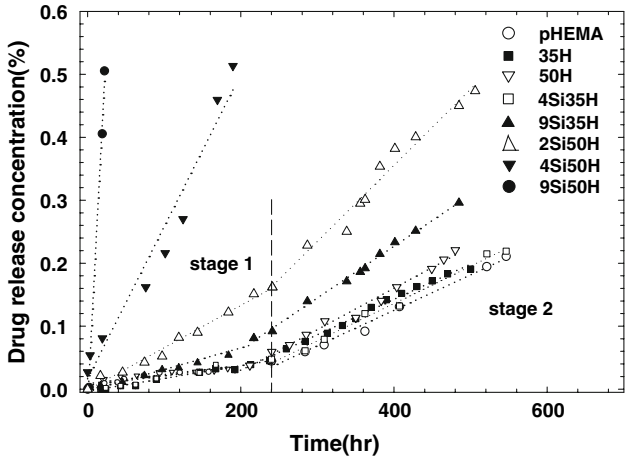

Fig. 7 Drug release profiles of pHEMA and SiO_2/pHEMA composites

of 2 types of water: free water and freezing bound water. The freezing bound water existing in the SiO_2/pHEMA composites may provide excellent compatibility with platelets. These analyses are consistent with the aforementioned observation that the addition of SiO_2 nanoparticles does exhibit slightly reduced platelet adhesion.

3.3 Drug release characterization

The drug release profiles of the pHEMA and SiO_2/pHEMA composites are shown in Fig. 7 wherein vitamin B_{12} was used as a model molecule. The release profiles of vitamin B_{12} for samples pHEMA, 35H, 50H, 4Si35H, 9Si35H, and 2Si50H showed a similar two-stage pattern consisting of a slow release in the first stage and a rapid release in the second stage. From the profile, the permeability of vitamin B_{12} is almost unchanged at the beginning but slightly increased in the second stage. Both stages follow a steady-state linear diffusion mode. The two-stage release profile may be attributed to the variation of the partition coefficient H that is a function of the concentration of the permeant dissolved in the membrane [31].

The partition coefficient is sensitive to the chemical and physical properties of both the permeant and the matrix system, including those of the polar groups and functional groups of the pHEMA and B_{12}, and the microstructure of the composite. However, it is difficult and impractical to differentiate the influence of individual characters on resultant drug release patterns; alternatively, these can be represented by the partition coefficient of the materials system. As illustrated in Table 2, the partition coefficient of the 0H, 35H, 50H, 4Si35H, 9Si35H, and 2Si50H samples shows a higher value in the second stage of drug release than in the first stage. This slight increase in the drug release rate in the second stage may be due to the complete swelling of the polymer matrix, corresponding to a higher diffusion rate. As evidenced in Fig. 8(a), sample 35H shows a dense structure before the swelling test; however, after approximately 20 days of the test, it became highly porous (Fig. 8(b)). The same scenario was also observed for samples 50H (Fig. 8(c)) and 9Si35H (Fig. 8(d)), wherein the latter showed the evolution of a greater number of completely swollen pores than that in the former. The variation in microstructural evolution is consistent with the drug diffusion characteristic in the second stage where the drug permeability of 9Si35H is higher than that of 35H and 50H. In addition, it was also noted in Fig. 7 that the addition of the silica nanoparticles increased the drug release rate in the second stage such as observed in the cases of 50H vs. 2Si50H and 35H vs. 9Si35H. One plausible explanation is that the evolution of these nanopores that underwent enlargement upon complete swelling created larger voids, enabling a greater number of drug

Table 2 The permeability [DH] of B_{12} of pHEMA and SiO_2/pHEMA composites

	Two-stage				Only one stage
	Stage 1		Stage 2		
	Permeability $[DH]_1$ (10^{-7} cm^2/hr)	Partition coefficient	Permeability $[DH]_2$ (10^{-7} cm^2/h)	Partition coefficient	Permeability [DH] (10^{-7} cm^2/h)
pHEMA	2.31	5.67×10^{-4}	4.22	8.72×10^{-4}	NA
35 H	2.39	6.72×10^{-4}	5.28	2.32×10^{-3}	NA
50 H	2.64	6.82×10^{-4}	5.75	3.88×10^{-3}	NA
4Si35H	2.71	7.12×10^{-4}	6.02	1.32×10^{-3}	NA
9Si35H	4.32	7.84×10^{-4}	8.14	5.27×10^{-3}	NA
2Si50H	7.29	6.87×10^{-4}	13.35	4.98×10^{-3}	NA
4Si50H	NA		NA		178
9Si50H	NA		NA		392

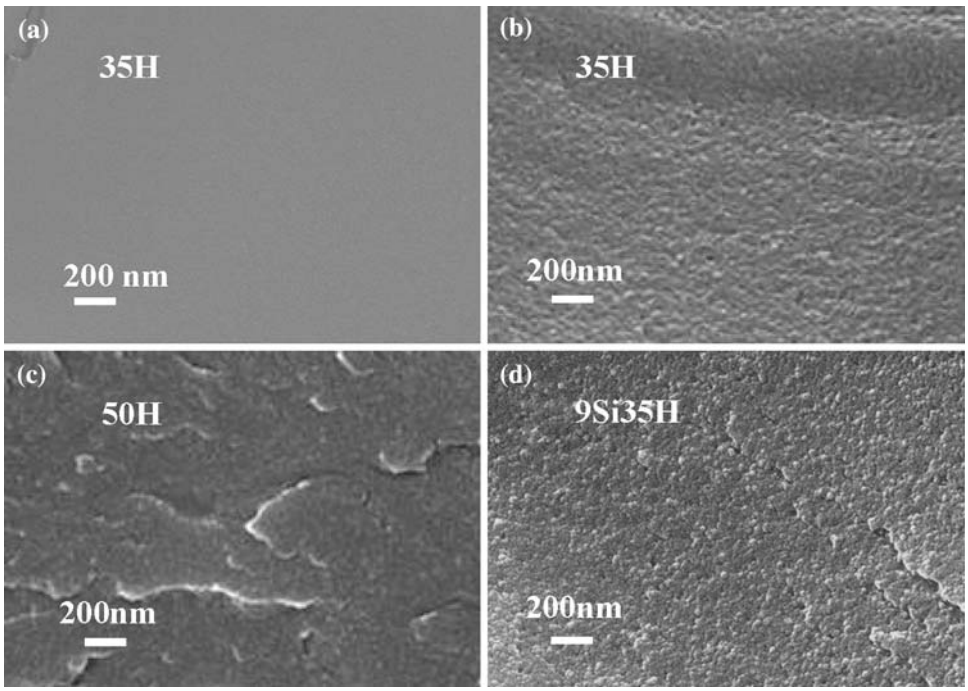

Fig. 8 SEM photographs of (**a**) 35H before drug diffusion and after drug diffusion for (**b**) 35H, (**c**) 9Si35H, and (**d**) 50H

molecules to diffuse into the environment. However, the presence of the SiO_2 nanoparticles does not appear to be an effective physical barrier for retarding drug diffusion through the composite membrane in these compositions.

In contrast, for samples with higher water incorporation during the course of synthesis, i.e., typically > 35%, the incorporation of a certain critical amount of the SiO_2 nanoparticles appeared to manipulate drug release, from a two-stage profile (samples 50H and 2Si50H) to a one-stage profile (samples 4Si50H and 9Si50H). Since a higher permeability [*DH*] was determined for samples 4Si50H and 9Si50H, which is similar to that observed for the second-stage profile of those samples, it is then believed that this one-stage release profile indicates that the release of drug is dominantly controlled by porosity. In other words, higher water and SiO_2 nanoparticles concentrations ensure a higher porosity of the resulting composites, rendering higher release rates and a corresponding higher permeability.

The influence of SiO_2 nanoparticles on the permeability of the resulting composites is illustrated in Fig. 9, with 35% and 50% water incorporation during the synthesis. The permeability of the Vitamin B_{12} increased linearly corresponding to the SiO_2 concentration when 50% water was incorporated during polymerization in the starting solution (i.e., 50H, 4Si50H, and 9Si50H). However, this permeability remains relatively unchanged with increasing concentrations of the SiO_2 nanoparticles for samples with 35% water incorporation. According to an earlier study, the critical water concentration for an effective phase separation should be greater than 35% for such an experiment,

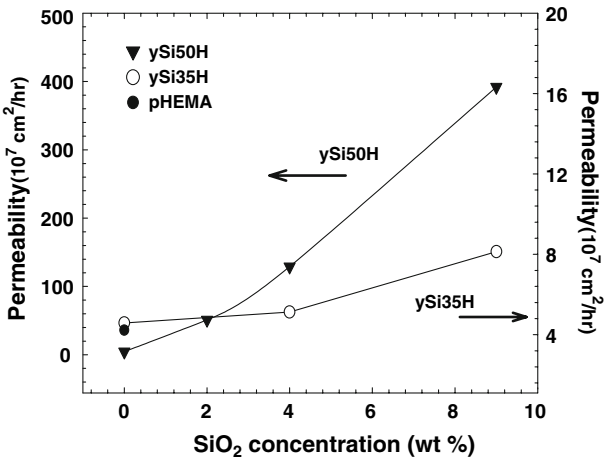

Fig. 9 Permeability [*DH*] of B_{12} at stage 2 of SiO_2/pHEMA composite

and the increase in nanoparticles, corresponding to an increase in nanoporosity, appeared to have little effect on the resultant drug diffusion. As shown in Fig. 10, the incorporation of SiO_2 nanoparticles increased the nanopore structure of the SiO_2/pHEMA composite. It was believed to be a compromise between the nanopore (as a diffusion conduit) and nanoparticle (as a physical barrier). However, higher water incorporation enhanced phase separation, which became more pronounced when the nanoparticles were introduced. This resulted in a more porous microstructure and thus enhanced drug diffusion.

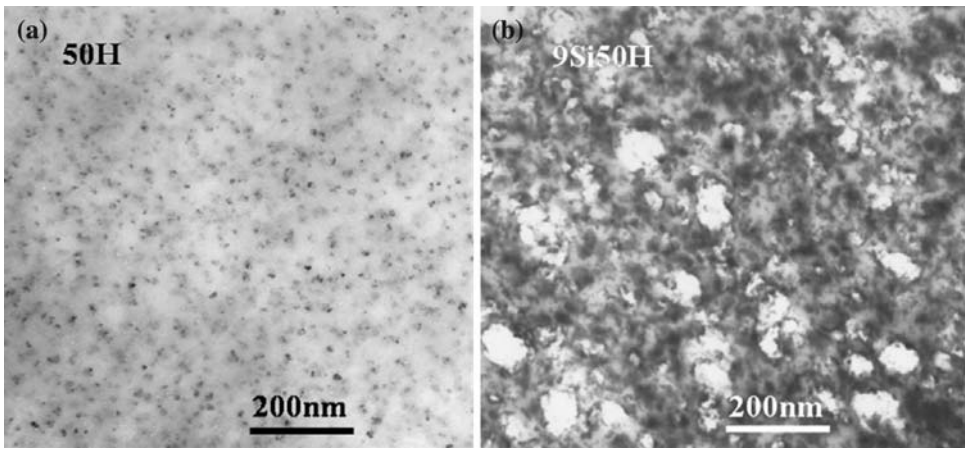

Fig. 10 TEM micrographs of SiO_2/pHEMA composite

4 Conclusions

Nanoporous SiO_2/pHEMA composites were prepared by the photopolymerization process. In comparison with neat pHEMA, the addition of SiO_2 nanoparticles revealed a significant effect on the reaction rate of crosslinking during polymerization, resulting in composites with varying nanoporous structures. The composites showed improved tensile strength, and the platelet adhesion property remained as excellent as that of neat pHEMA, which encourages the use of such composites for antithrombotic applications. Drug diffusion characteristics in the composites can be well modulated by controlling the concentrations of the SiO_2 nanoparticles and water in the starting stage of synthesis. By taking into consideration the aforementioned improved properties, it is suggested that the nanoporous SiO_2/pHEMA composites can be employed as candidate biomaterials for coatings or as bulk devices for a number of biomedical applications.

Acknowledgements The authors would like to thank the National Science Council of the Republic of China for its financial support through Contract No. NSC-95-2216-E-009-027. We also thank the Chinese Blood Donation Association of Hsinchu for their technical assistance.

References

1. C. Ohtsuki, T. Miyazaki, M. Tanihara, Mater. Sci. Eng. C-Biomimetic Supramol. Syst. **22**, 27 (2002)
2. A.K. Bajpai, D.D. Mishra, J. Mater. Sci. Mater. Med. **15**, 583 (2004)
3. J. Song, E. Saiz, C.R. Bertozzi, J. European Ceram. Soc. **23**, 2905 (2003)
4. R. Di Maggio, L. Fambri, R. Campostrini, J. Sol-Gel Sci. Technol. **26**, 339 (2003)
5. P. Hajji, L. David, J.F. Gerard, J.P. Pascault, G. Vigier, J. Polym. Sci. Pt. B-Polym. Phys. **37**, 3172 (1999)
6. M. Aparicio, J. Mosa, A. Duran, J. Sol-Gel Sci. Technol. **40**, 309 (2006)
7. N.H. Park, K.D. Suh, J. Appl. Polym. Sci. **71**, 1597 (1999)
8. R.O.R. Costa, M.M. Pereira, F.S. Lameiras, W.L. Vasconcelos, J. Mater. Sci.-Mater. Med. **16**, 927 (2005)
9. R.O.R. Costa, W.L. Vasconcelos, J. Non-Cryst. Solids **304**, 84 (2002)
10. S.L. Huang, W.K. Chin, W.P. Yanga, Polymer **46**, 1865 (2005)
11. T. Suzuki, Y. Mizushima, T. Umeda, R. Ohashi, J. Biosci. Bioeng. **88**, 194 (1999)
12. B.A. Weisenberg, D.L. Mooradian, J. Biomed. Mater. Res. A **60**, 283 (2002)
13. H.M. Chen, X.M. Tian, H. Zou, Artif. Cells Blood Substit. Biotechnol. **26**, 431 (1998)
14. C.C.-Y. Lee, J.E. Mark, P.A. Bianconi, *Hybrid Organic-Inorganic Composites* (American Chemical Society, Washington, DC, 1995)
15. G.W. Scherer, C.J. Brinker, *Sol–Gel Science* (Academic Press, New York, 1989)
16. M.C. Yang, T.Y. Liu, J. Memb. Sci. **226**, 119 (2003)
17. M. Miyajima, A. Koshika, J.I. Okada M. Ikeda, J. Control. Release **60**, 199 (1999)
18. S.X. Lu, K.S. Anseth, J. Control. Release **57**, 291 (1999)
19. J.D. Cho, H.T. Ju, J.W. Hong, J. Polym. Sci. Pol. Chem. **43**, 658 (2005)
20. D.S. Kim, K.M. Lee, J. Appl. Polym. Sci. **92**, 1955 (2004)
21. J.E. Elliott, J.W. Anseth, C.N. Bowman, Chem. Eng. Sci. **56**, 3173 (2001)
22. M. Taira, H. Suzuki, H. Toyooka, M. Yamaki, J. Mater. Sci. Lett. **13**, 68 (1994)
23. W.S. Kim, Y.C. Jeong, J.K. Park, Opt. Express **14**, 8967 (2006)
24. P. Bosch, F. Delmonte, J.L. Mateo, D. Levy, J. Polym. Sci. Pol. Chem. **34**, 3289 (1996)
25. F. Branda, A. Costantini, G. Luciani, L. Ambrosio, J. Biomed. Mater. Res. A **57**, 79 (2001)
26. S.M. Murphy, C.J. Hamilton, B.J. Tighe, Polymer **29**, 1887 (1988)
27. A. Barnes, P.H. Corkhill, B.J. Tighe, Polymer **29**, 2191 (1988)
28. M. Tanaka, A. Mochizuki, J. Biomed. Mater. Res. A **68A**, 684 (2004)
29. M. Tanaka, A. Mochizuki, N. Ishii, T. Motomura, T. Hatakeyama, Biomacromolecules **3**, 36 (2002)
30. E. Hirota, K. Ute, M. Uehara, T. Kitayama, M. Tanaka, A. Mochizuki, J. Biomed. Mater. Res. A **76A**, 540 (2006)
31. R. Baker, *Controlled Release of Biologically Active Agents* (Wiley, New York)